INTERNATIONAL JOURNAL OF LATEST TECHNOLOGY IN ENGINEERING, MANAGEMENT & APPLIED SCIENCE (IJLTEMAS)

ISSN 2278-2540 | DOI: 10.51583/IJLTEMAS | Volume XIII, Issue V, May 2024

Structural Characterization of High Resolution Aeromagnetic Data for Potentially Mineralized Zones Identification Within the North-Central Basement Complex of Nigeria

***Bwamba Jonah Ayuba, Abu Mallam and Abel Osagie**

Physics Department, University of Abuja, Abuja

***Corresponding Author**

DOI: https://doi.org/10.51583/IJLTEMAS.2024.130703

Received: 04 June 2024; Revised: 02 July 2024; Accepted: 10 July 2024; Published: 26 July 2024

Abstract: The aim of this study is to identify mineralization zones within the North-Central Basement Complex of Nigeria. The goal was to locate important geological formations and assess the region's suitability for mining exploitation. Several filters were used to enhance the short wavelength anomalies which could give preliminary information about the magnetic minerals present in the study area which spans latitudes 8°00'N to 9°30'N and longitudes 6°30'E to 7°30'E. The total magnetic intensity map revealed overall field strengths ranging from -99.63 nT to 109.33 nT. The filters used are fisrt horizontal and vertical derivatives, analytic signal and 3-D Euler Deconvolution. The first horizontal and first vertical derivatives show structures like lineament that could host to minerals present in the study. The Analytic Signal processing highlighted three distinct magnetic anomaly zones: a low zone (0.004 nT/m to 0.013 nT/m), an intermediate zone (0.016 nT/m to 0.048 nT/m), and a high zone (0.057 nT/m to 0.282 nT/m). The horizontal derivative map displayed both positive and negative anomalies, with values ranging from -0.061 to 0.061 nT/m. The Euler depth analysis suggested the magnetic sources are located at depths greater than 2000 m, between 1000-2000 m, 500-1000 m, and less than 500 m. The lineament map revealed a dominant NE-SW trend, with a less dominant E-W and NW-SE trend within the study area. The high lineament density areas of Kwali, Gwagwalada, Shanzhi, Dadabiri, Checheyi, Pangu, and Suleja correspond to the various mineralization zones identified in the region.

Keywords: Mineral, Characterization, Basement, Complex, Aeromagnetic

I. Introduction

The analysis of aeromagnetic maps entails the interpretation of underlying rock formations and a thorough investigation of structural and lithological changes within the subsurface. The magnetic basement refers to a collection of rocks that lie beneath sedimentary basins and may occasionally be exposed at certain locations (Onyedim et al, 2007). Surface linear features can often be observed on aeromagnetic maps, indicating the presence of magnetic anomalies in numerous sedimentary basins. These anomalies result from the secondary mineralization occurring along fault planes.

The exploration of solid minerals is a worldwide occurrence, and numerous scientists have employed different techniques and methods in various places to accomplish their objectives. The choice of method to be utilized is often influenced by the nature of the deposits. For example, Guo et al. found that in two separate locations within China's Gansu Province, the ground magnetic method effectively detected the presence of gold minerals connected to sedimentary layers and sulfides, including pyrrhotite.

However, the magnetic technique proved unsuccessful in identifying mineralization at the third site within the same region. This was due to the magnetic signal being obstructed by the response of the igneous host rock, thereby preventing the detection of mineralization. Hence, it is essential for a researcher to have a thorough understanding of the geological characteristics of the study area in order to determine the most appropriate geophysical technique to utilize. Mohamed et al. (2017) used a combination of these processing techniques to analyze aeromagnetic data and extract valuable information about the subsurface geology. Each technique has its own advantages and limitations, and their integration allows for a more comprehensive understanding of the magnetic anomalies and geological features present in the study area.

Other researchers such as Priscillia, *et al.*, (2021), Arifin *et al.* (2019), Andrew *et al*. (2018), Adetona *et al.* (2013), Abdulsalam et al. (2011), Arinze *et al*. (2018), Ejepu *et al*. (2020) and Oguche *et al.*, (2021) have applied different aeromagnetic analytical techniques to delineate mineralized zones in various locations across Nigeria. These researchers were able to discover numerous new occurrences, including lineaments that could serve as hosts for minerals.

Despite being endowed with a variety of mineral resources tucked away beneath the earth's surface, Nigeria is entirely dependent on crude oil (Obaje, 2009). Solid minerals are not effectively used for the benefit of the nation's economy. The volatile price of crude oil greatly impacts the economy of Nigeria, and given that the hydrocarbon reservoir of the abundant Niger Delta is being drained or may soon run out as a result of ongoing exploitation, the focus needs to be directed into other areas. Investigating our readily available natural resources is a logical approach toward diversifying Nigeria's economy. Local miners have widely exploited natural resources illegally and in an unprofessional manner in several locations of Nigeria. However, to accurately determine the quantity, types, and depth of these mineral deposits, the government has not done far much in carrying out the geophysical investigation that is required.

ISSN 2278-2540 | DOI: 10.51583/IJLTEMAS | Volume XIII, Issue V, May 2024

This puts mining operations in the hands of unlicensed miners who are ignorant of the resources found underneath the surface of the earth. The economy, safety, health, and ecology of the nation are all impacted by the operations of these local miners. Geophysical surveys face challenges due to mineralization due to complicated geology and structure, which prevents some of the mineralization from providing a contrast with the host geology that can be identified by any of the geophysical parameters (Hodges and Amine, 2010).

The research was aimed at delineating and characterizing subsurface geologic structures that could host possible minerals in the study area using different filter applications.

Location and Geology of Study Area

The study area is part of Nigeria's North-Central Basement Complex and covers longitude 6° 30' to 7° 30'E and latitude 8° 00′ to 9°30′N with an estimated area of 18000 km^2. and falls within the area under stud According to Abaa (1983), the Basement Complex of Nigeria can be regionally categorised into four (4) major lithological units namely; the Migmatites-Gneiss Complex, Schist belt (Metasedimentary and Metavolcanics rocks), Older Granites (Pan African Granitoids) and Undeformed Acid and Basic Dykes (Fig.1).

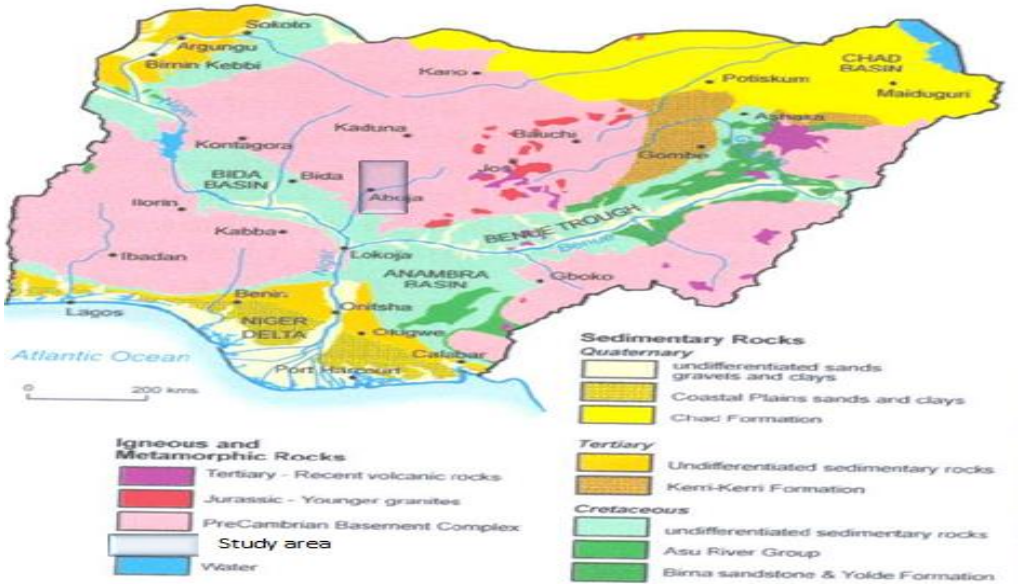

Fig. 1 Geological map of Nigeria showing the study area modified after NGSA (2010).

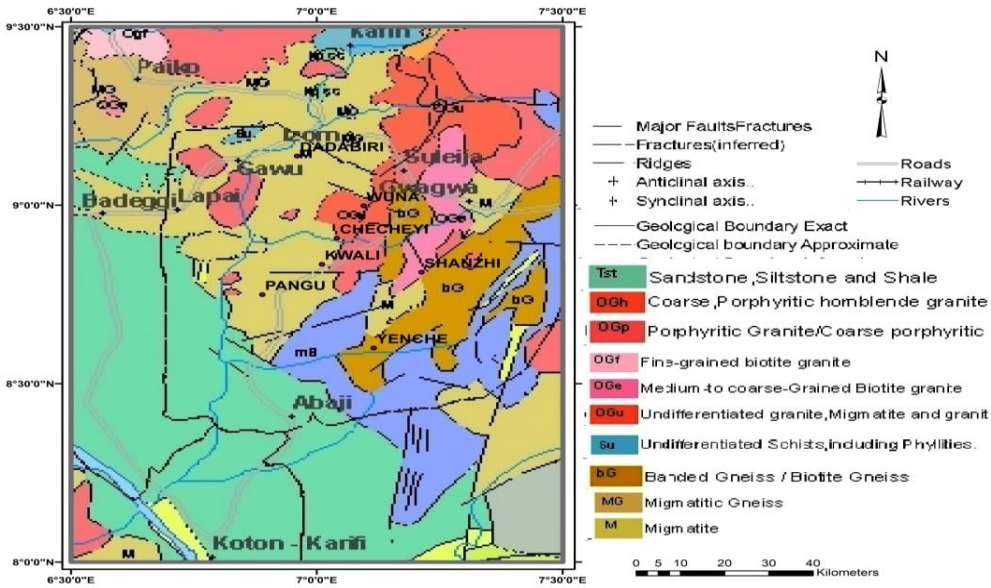

Fig. 2: Map showing the geological distribution of the site, modified from NGSA (NGSA, 2006)

According to reports, a diverse range of mineral resources, such as iron ores and gold have been discovered in the region, Burke et al. (1976). The study area is characterized by the presence of migmatitic Precambrian basement rocks, Proterozoic

ISSN 2278-2540 | DOI: 10.51583/IJLTEMAS | Volume XIII, Issue V, May 2024

metasedimentary belts (schist), granitoids, and tertiary sediments (fig. 2). The site contains a variety of rocks in its Precambrian basement, including sheared rocks, migmatite, migmatitic gneiss, banded gneiss, and granite gneiss. Additionally, the Proterozoic metasedimentary belts consist of schist (undifferentiated), phyllite, and slate. The Basement Complex and the sedimentary rocks found in the Middle Benue and Northern Anambra Basins are the two main components of the geological makeup of the research area, as described by Obaje (2009). Low-grade metasediments predominate in the N-S trending belts that make up the Schist Belts, which are primarily located in the western part of Nigeria, according to Dada (2006). The main constituents of these belts are supracrustal rocks from the Upper Proterozoic that have been folded inside the migmatite-gneiss complex. The schist belts exhibit a variety of lithological features, such as amphibolites, pelitic schists, phyllites, banded iron formations, carbonate rocks including marbles and dolomitic marbles, and clastics with different grain sizes. In the study area, the Zungeru, Igara and Muro Hills Schist Belts are most prominent in Niger, Kogi and Nasarawa States respectively

The schist belts located in northcentral Nigeria that were captured within the study area constitute the principal ones. This is mostly found around north and east of Abaji, extending northward towards the southern part of Yenche and east of Shanzhi.

II. Materials and Methodology

The methods employed in this research involved knitting appropriately six (6) aeromagnetic data sheets (185, 186, 206, 207, 227 and 228) obtained from Nigerian Geological Survey Agency (NGSA) which cover a total area of about 18,000 km^2 to form a single database for the study which was used to produce the Total Magnetic intensity (Fig. 3). The magnetic inclination (− 0.36) and declination (− 1.83) were obtained based on the International Geomagnetic Reference Field (IGRF) 2005 on the magnetic calculator to generate the reduction to the magnetic equator (RTE) map (Fig. 3) by employing the use of Oasis Montaj software. The RTE transformation focuses on aligning the peak of the magnetic anomalies with their underlying magnetic sources, thereby removing any unevenness associated with magnetic anomalies at low latitudes and the influence of magnetic inclination (Oyeniyi et al., 2016; Glbert and Gideano, 1985).

The data were captured for NGSA from 2005 to 2010 by Fugro Airborne Surveys as part of nationwide airborne geophysical surveys and were acquired along a series of NE–SW profiles with a flight line spacing of 500 m and terrain clearance of 80 m. This was followed by application of various enhancement filters on the TMI-RTE grid such as Analytic Signal to detect the edges the bodies present and depth, Euler Deconvolution technique to ascertain the location and depth of the structure, Center for Exploration Targeting grid analysis to reveal the lineaments which could serve as potential host for mineralized deposit in the study area. Other enhancement filters like the vertical, horizontal and tilt derivatives have similarly been used in delineating shallow basement structures or geological boundaries such as lineaments, cracks, fractures, faults, etc.

Total Magnetic Intensity Reduction to the Equator (RTE)

The inclination and declination angles of the geomagnetic field determine the form of magnetic anomalies caused by vertical bodies in the geomagnetic procedures. The main field plunges vertically in the north and south magnetic poles, and symmetric magnetic anomalies are shaped with the maximum or minimum precisely over the causative magnetic body. Because the magnetic signature of magnetized things at low latitudes is usually bipolar, it is difficult to match the observed anomalous maxima with the placements of sources at low magnetic latitudes (between 15°S and 15˚N). Researchers vary the analytical maps in the space domain, as is the case with the reduction-to-the-equator (RTE), to make it easier to explain the anomalies at very low latitudes. The magnetic data can be reduced to the equator (RTE) according to Leu (1982), to make the magnetic bodies appear horizontal. Since the study area is located within low-magnetic latitudes (i.e., areas with geomagnetic inclination less than 15°), where a satisfactory reduction to the pole (RTP) of magnetic data is not possible, and the TMI grid data were then transformed using the RTE filter rather than the reduction to the pole filter. In order to modify and accentuate magnetic anomalies connected to the boundaries of surface and near-surface geological bodies, structures, and depths, the TMI-RTE grid data for the region were processed.

The RTE filter is represented mathematically by equation (1) (Bhattachanya, 1966).

$$L(\theta) = \frac{[\sin(I) - i\cos(I).\cos(D-\theta)]^2\left(-cos^2(D-\theta)\right)}{[sin^2(Ia) + cos^2(Ia).cos^2(D-\theta)].[sin^2(I) + cos^2(D-\theta)]}\ if\ \langle I_a| < |I\rangle, I_{a=I} - - - 1$$

where, I= Geomagnetic Inclination, D= Geomagnetic Declination and $L(\theta)$= Directions of the wavenumber vector in degrees of azimuth.

Analytic Signal

Nabighian (1972, 1974) presented the idea of the analytic signal for mathematical interpretation and demonstrated how its amplitude produces a function with a bell shape over each corner of a two-dimensional body with a polygonal cross section. The depth of a contact can be determined by the width of an anomaly, as long as the signal from a single point of contact can be detected. This method is particularly useful at low magnetic latitudes and is commonly employed for reduction to pole data. Moreover, even data that has not undergone reduction to pole can still yield the desired outcome when applying the method, as the anomalies are usually accurately positioned above the causal bodies (Tsepav 2020). The analytic signal (AS) utilizes the magnetization properties, including strength and direction, of inclined magnetizing bodies to transform their shapes and

ISSN 2278-2540 | DOI: 10.51583/IJLTEMAS | Volume XIII, Issue V, May 2024

symmetrically align the peaks over their sources. This technique effectively displays the amplitude strength of litho-structural features by highlighting their magnetization contrast. It serves as a valuable tool for mapping and classifying litho-structural characteristics, as described by MacLeod et al. (1993). Roest *et al* (1992) showed that the amplitude of the three dimensional analytic signal at location (x, y, z) can be derived from the three orthogonal gradients of the total magnetic field using the equation:

$$|A(x,y,z)| = \left[\left(\frac{dT}{dx}\right)^2 + \left(\frac{dT}{dy}\right)^2 + \left(\frac{dT}{dz}\right)^2\right]^{\frac{1}{2}} \text{----------2}$$

where $|A(x,y,z)|$ is the amplitude of the analytic signal at (x, y, z).

First Horizontal and First Vertical Derivatives

The horizontal and vertical derivatives suppress the long wavelengths, which are deeper sources and regional features, and enhance the shallow wavelength features, which are the product of near surface structures obscured by stronger effects of broader regional features. First Vertical Derivative, FVD (Fig. 5) and First Horizontal Derivative, FHD (Figure 6) involve the process of taking the derivative of the magnetic field data with respect to the vertical and horizontal direction respectively. According to the references cited (Salem et al., 2007 and Okpoli & Akingboye, 2016), the tilt derivative has the ability to enhance both weak and strong magnetic anomalies by placing the anomaly directly over its source. Mathematically, the Vertical derivative is defined as:

$$L(\mu) = (\mu i)^n \text{ ----------3}$$

Where μ is the x component of the wavenumber, $i = \sqrt{-1}$ and *n* is the order of differentiation while the horizontal component is represented mathematically by the algorithm:

$$L(V) = (Vi)^n \quad \text{----------4}$$

where *V* represents the y component of the wavenumber, $i = \sqrt{-1}$ and *n* is the order of differentiaton.

Tilt derivative is the arctan of the ratio of vertical derivative to the horizontal derivative,

$$\theta = \tan^{-1}\left(\frac{\partial A/\partial z}{\partial A/\partial h}\right), \text{ ----------5}$$

where the numerator and denominator are vertical and horizontal derivatives of the anomaly, respectively, the latter given by

$$\partial A/\partial h = \sqrt{(\partial A/\partial x)^2} + \sqrt{(\partial A/\partial y)^2} \text{ ----------6}$$

Centre For Exploration Targeting (CET) Grid Analysis

The Centre for Exploration Targeting **(**CET) Grid Analysis extension for Oasis Montaj consists of a number of tools that provide automated lineament detection of gridded data, which can be used for first-pass data processing. These tools provide a rapid unbiased workflow that reduces the time with which one can interpret gridded data. The method contains tools for texture analysis, phase analysis, and structure detection which are versatile algorithms useful for grid texture analysis, lineament, edge and threshold detection. It utilizes standard deviation, which provides an estimation of the local variation in the data. It calculates the standard deviation of the values within the local neighbourhood of each location in the grid, revealing features of significance which often exhibit high variability with respect to the background signals. The standard deviation σ of the cell values x_i for a window of N cells whose mean value is μ is given as:

$$\sigma = \sqrt{\frac{1}{N}\sum_{i=1}^{N}(x_1 - \mu)^2} \quad \text{----------5}$$

3.5 3D Euler Deconvolution

Euler deconvolution's technique is an equivalent method based on the Euler's homogeneity equation as developed by Reid *et al.* (1990) following Thompson's (1973) suggestion and operating on gridded magnetic data. These Euler depth solutions not only estimate the depth, but also delineate the horizontal boundaries, Wilsher (1987). In a general case, scattered data points cannot provide superior solutions. Various researchers have used 3D Euler deconvolution technique for source depth estimations (Nabighian, et al., 2001). The method is based on the concept that anomalous magnetic fields of localized structures are homogeneous function of the source coordinate and, therefore, satisfies Euler's homogeneity equation. Usually the structural index

(SI) is fixed and the locations and depths (x_0, y_0, z_0) of any sources are found using the following equation:

$$\frac{\partial f}{\partial x}(x - x_0) + \frac{\partial f}{\partial y}(y - y_0) + \frac{\partial f}{\partial z}(z - z_o) = SI(B - f) \text{ ----------6}$$

where f is the observed field of location $(x, y \text{ and } z)$ and *f* is the base level of the field [regional value at the point (*x*,*y*,*z*)] and *SI* is the structural index or degree of homogeneity

ISSN 2278-2540 | DOI: 10.51583/IJLTEMAS | Volume XIII, Issue V, May 2024

III. Results and Discussion

The interpretation of aeromagnetic data requires drawing conclusions about the geology of a region from the pattern of observed magnetic signatures. Because magnetic minerals are important in the mineralization process, aeromagnetic survey can be used to map the geology of a region; boundaries in magnetic properties are frequently correlated with lithological boundaries (Reeves 2005).

Total Magnetic Intensity Map

Positive anomalies are depicted by magenta and red shades, while negative anomalies are represented by light and dark blue hues. These anomalies, characterized by low magnetic amplitudes, are believed to be related to the Formation of Bida basin, similar to the Patti formation. Authors like Ladipo (1988), Nwajide (1990), Pettijohn (2004), and Akande et al. (2006) reported that these areas consist of sedimentary rocks such as clay stones, silt stones, limestone, and interbedded shale. Fig. 3 shows the overall strength of aeromagnetic intensity, ranging from -99.63 nT to 109.33 nT.

The map reveals negative features which is broadly seen in the southwestern part of the study area. These negative anomalies are also visible around Suleja, Checheyi, Zuba, east of Dadabiri, south of Gwarinpa, the area around latitude N9°00′ and areas around the far north-eastern corner of the area of study. The negative values range between - -99.63 nT and 10.47 nT. Strong magnetic anomalies are also observed with the highest value peaking at 109.33 nT. These positive anomalies are observed to be trending in the NW-SE direction. These strong magnetic anomalies can be visibly noticed around west of Dadabiri, north of Pangu, Yenche, west of Kwali, southwest of Abaji and the northern part of Suleja. The map reveals strong correlation between regions of high magnetic anomalies and locations of mining pits within the area of study. These regions of strong magnetic anomalies can be observed in fig. 2 to correspond geologically with migmatite, migmatitic gneiss, banded gneiss/ biotite gneiss and undifferentiated schists including phylitties assemblages.

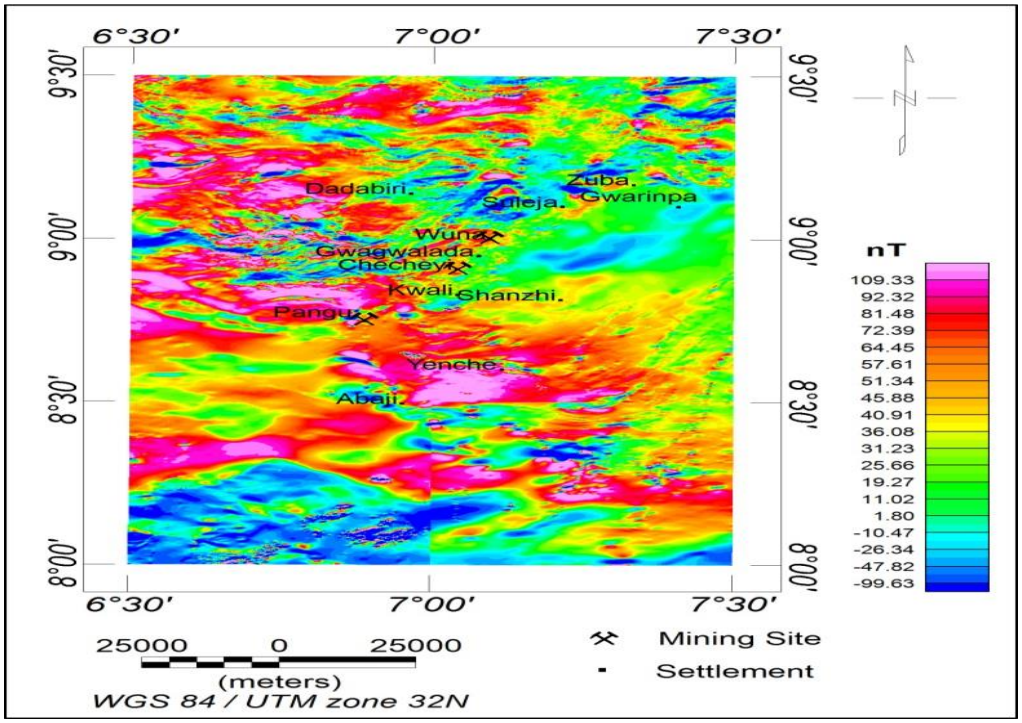

Fig.3: Total Magnetic Intensity map of the study area.

Total Magnetic Intensity Reduction to the Equator (TMI-RTE) Map

In order to properly map and delineate inclined and other aligned forms of structures, the TMI-RTE image (Fig. 4) is created by centering the peaks of magnetic anomalies on their sources based on the inclination and declination of the local field of the magnetizing body.

Using Oasis Montaj program v8.4, the entire Intensity Magnetic Map (Fig. 3) is reduced to the equator. Fig. 2 and fig. 4 depict litho-structural similarities between the geological map and the RTE_TMI image. The severely distorted rocks in the region clearly match the Migmatite-Gneiss Complex because they show evidence of both positive and negative intensity values, which ranged from -101.98 to 101.69 nT. These abnormal variations in the rocks are linked to ferromagnetic minerals, which frequently result in extremely high magnetic intensities, strong degrees of metamorphism, and deformities that yield low and negative intensity values. The area of study can be divided into four magnetic zones on the TMI-RTE map, each of which has a distinct magnetic anomaly pattern.

ISSN 2278-2540 | DOI: 10.51583/IJLTEMAS | Volume XIII, Issue V, May 2024

The first zone occupies the southwestern (south of Abaji), northeastern (Suleja and Zuba) and southeastern parts of the area. This is also observed to occupy the northeastern and southeastern fringes of the study area and is underlain by the Precambrian crystalline basement rocks (migmatites, sandstones, siltstones, shale and porphyritic granites). It is distinguished by extremely low wavelength (low wavenumber) anomalies (bright and dark blue colors), with a magnetic intensity amplitude ranging from -101.98 nT to -14. nT. The second magnetic anomalies zone has its values ranging from -1.02 nT to 27.96 nT. This zone shows positive anomalies which are distinguishable by low magnetic values. These low values are observed around south of Gwarinpa (areas around latitude 9º00'N), the northern part of Zuba and the areas around latitude 8º30'N (west of Abaji). This is also noticeable around the southeastern part of the study area extending to southeastern part of Abaji. These areas are characterized by the presence sanbstone, siltstone shale, medium to fine and coarse-grained biotite granite (fig. 2). The third region comprises of anomalies ranging from 33.16 nT to 59.33 nT (light yellow to red coloration). This region is noticeable around Shanzhi and the adjoining areas, Kwali, Pangu, north of Yenche, Dadabiri and southwest of Abaji. The zone represents transition between sedimentary and basement complex zones of the lower Bida basin. The fourth zone occupies the northwestern (north of Pangu, west of Kwali, west of Dadabiri and the extreme north) and central (Yenche) part of the study area. This zone is characterized by very high magnetic anomalies values ranging from 66.40 nT to 101.69 nT. The areas are geologically underlain by sanbstone, siltstone, shale, migmatic gnesis and banded gnesis/biotite gnesis. The high anomalies are oserved to be trending in mainly in the NW-SE direction.

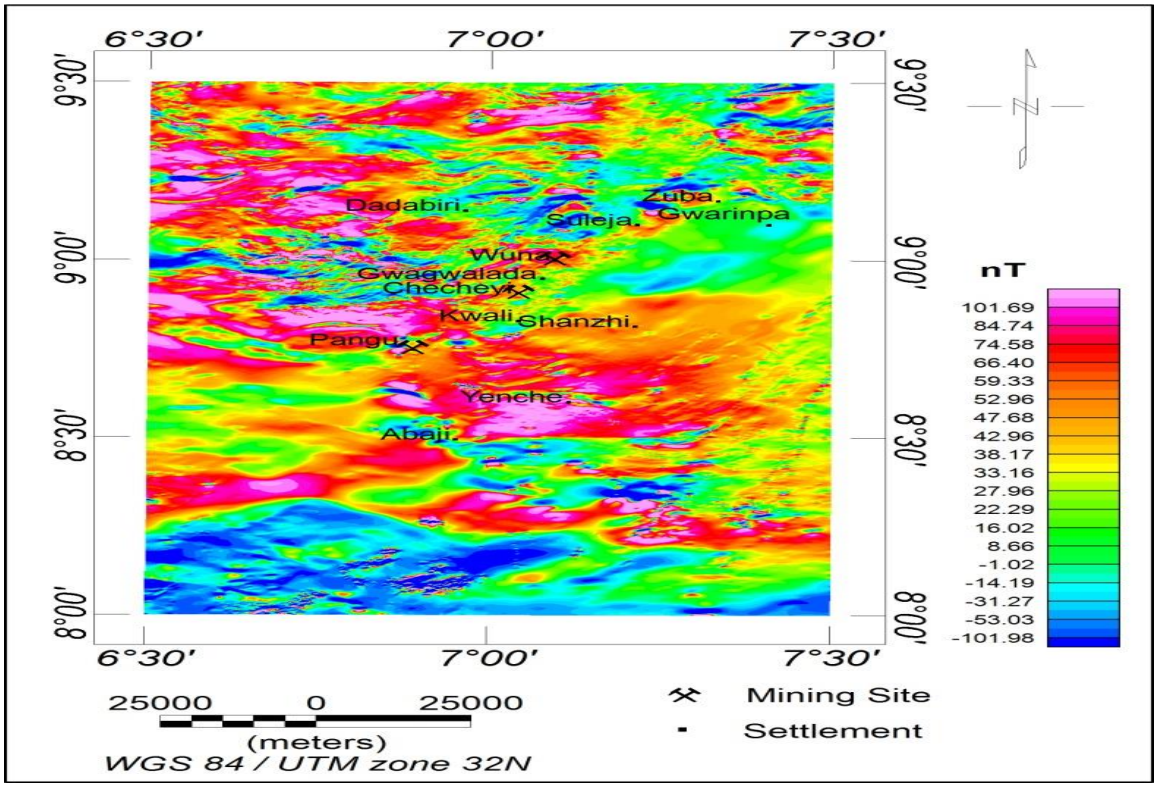

Fig. 4: RTE map of the study area.

Analytic Signal map

By altering the inclined magnetizing bodies' forms based on the direction of geologic strike with respect to the magnetization vector, the analytic signal (AS) focuses the peaks of the magnetizing bodies uniformly over their origins. Based on the magnetization of various rock compositions, the Analytic Signal map (fig. 5) displays all the edges of anomalous occurrences, structural patterns, and lithological contacts, (Faruwa et al. 2021 and Lawal, 2020). This has suggested the characterization of the study area into three magnetic anomalies zones: the low zone (0.004 nT/m to 0.013 nT/m), the intermediate zone (0.016 nT/m to 0.048 nT/m) and the high zone (0.057 nT/m to 0.282 nT/m). The geologic units (undifferentiated schists, granite gneiss, biotite gneiss, migmatite, and migmatite gneiss) around Gwagwalada, Kwali and Wuna can be said to be responsible for the very high magnetic anomalies with the study area. This strong signal amplitude also corresponds with that of the mining sites of Pangu, Wuna and Checheyi, an indication that these minerals are structurally controlled. The younger metasediments, like the phyllites, are represented within the intermediate zone. The low magnetic zones (areas south of Pangu, west and south of Abaji, south of Gwarinpa and the region around latitude 8º45'N to 9º00'N and longitude 7º15'E to 7º30'E) correspond to the sedimentary terrains consisting of clay, pebbles, and sandstones. Arewa and Fahad (2024) obtained (> 0.094 nT/m), (0.028 to 0.094 nT/m) and (< 0.028 nT/m) as high, intermediate and low zones respectively in the north-western part of Nigeria.

ISSN 2278-2540 | DOI: 10.51583/IJLTEMAS | Volume XIII, Issue V, May 2024

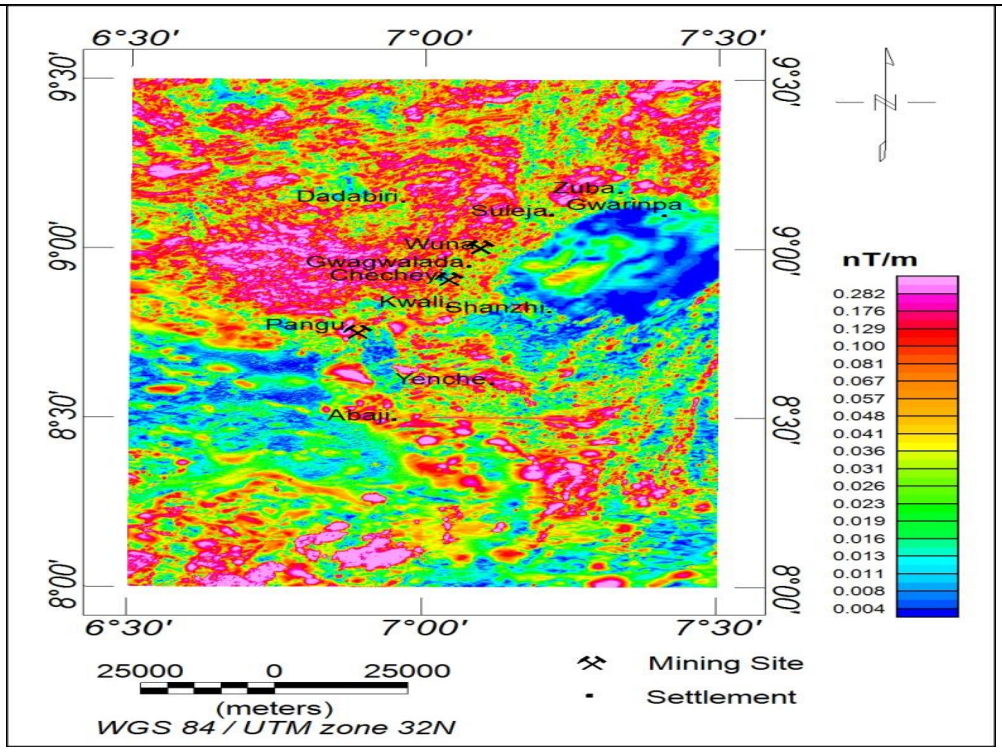

Fig. 5: Analytic Signal map of the study area.

Horizontal and Vertical Derivatives maps

The first vertical derivative map (fig. 6) has been successful in showcasing the short wavelength magnetic characteristics and capturing long wavelength geologic features. The magnetic intensities of structures around the mining sites range from 0.003 to 0.0112nT/m which corresponds with sediments with thicker formations.

The horizontal derivative map displays both positive and negative anomaly with values ranging from -0.061 to 0.061 nT/m as shown in fig. 7.

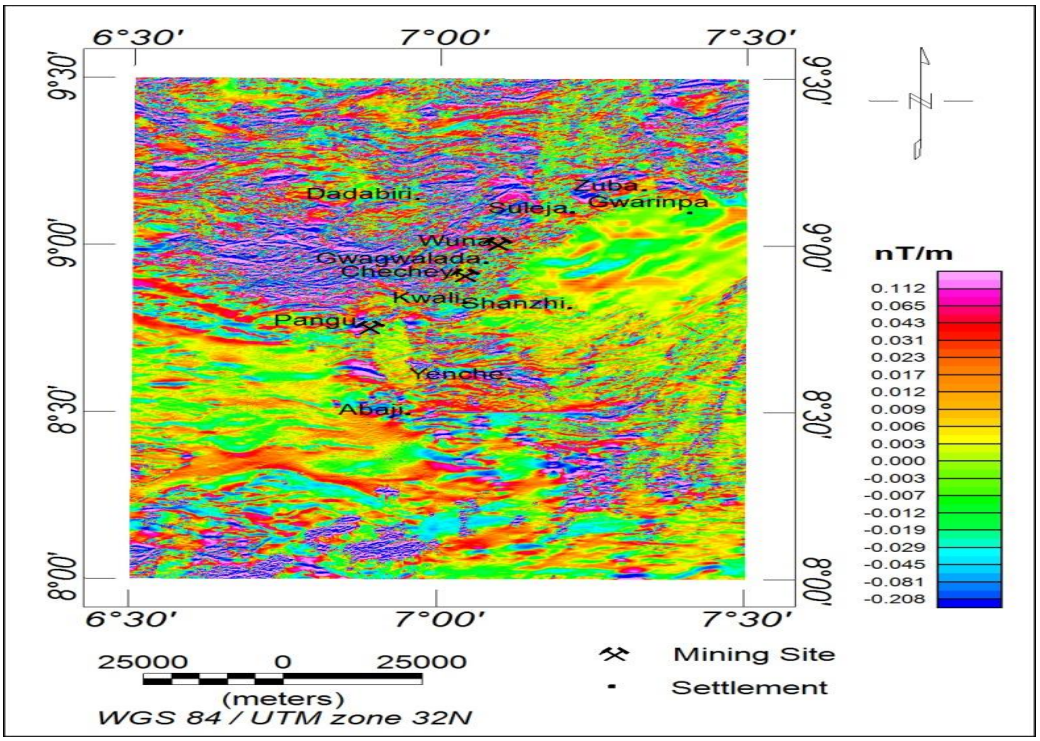

Fig. 6: First Vertical Derivative map of the study

ISSN 2278-2540 | DOI: 10.51583/IJLTEMAS | Volume XIII, Issue V, May 2024

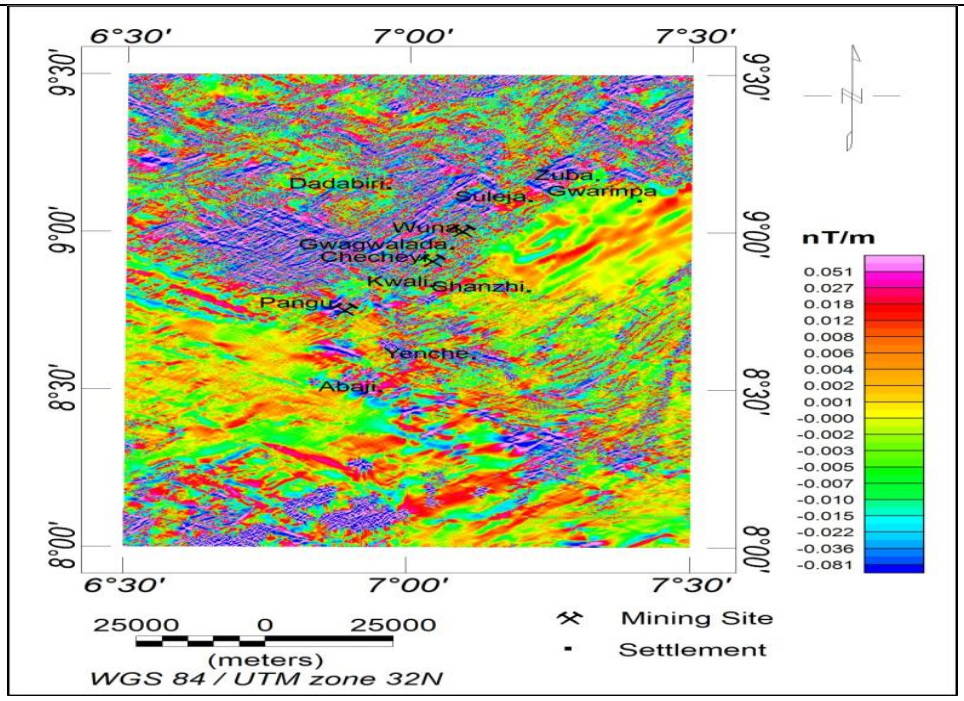

Fig. 7: First Horizontal Derivative map of the study

3-D Euler Deconvolution (ED) Map

In this study the 3-D Euler Deconvolution technique has been applied to the TMI_RTE grid data of the study area to characterize depth and location of basement rock contact (faults or dykes) at structural index of one (SI=1) which conforms with what Reid, et al (1990) have reported. The result of the Euler depth shows the depth of magnetic sources range to be >2000 m, 1000 to 2000 m, 500 to 1000 m, and < 500 m. Most of the highly magnetic structures and intrusive depth sources are within the range of < 100 to 500 m (Fig. 8). The depth estimation of mineralization potential sources around the mining sites of Pangu, Checheyi and Wuna in the central part of the study area is found to be <500 m which is in agreement with the result of Analytic Signal, the FVD, FHD and CET structural maps.

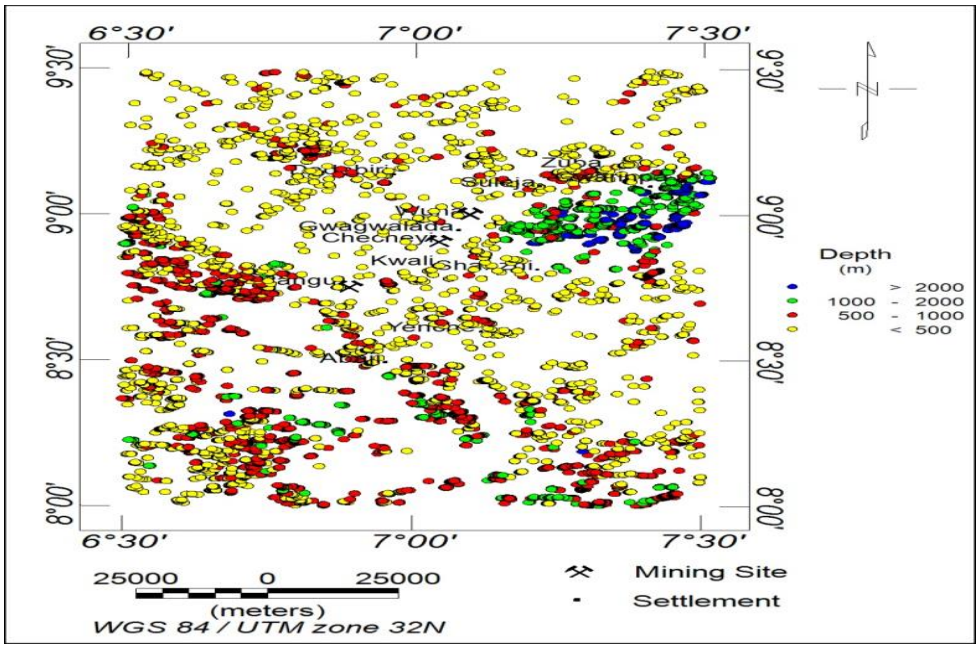

Fig. 8: 3D Euler deconvolution depth solution.

Lineament map

The lineaments derived from aeromagnetic images were evaluated based on their length and orientation, so investigating their spatial arrangement in order to better illustrate the faults in the study area and obtain additional insight into the distribution and

ISSN 2278-2540 | DOI: 10.51583/IJLTEMAS | Volume XIII, Issue V, May 2024

presence of lineaments. Fig. 9 shows the concentration of these structures predominantly in the northern half of the study area. An analysis of the structures for the orientation was carried out and plotted as rose diagram (Fig.10). The predominant directional patterns are shown as E-W, NE-SW, and W-NW to E-SE in Fig. 10. Authors like Holden, et al. (2008), Faruwa, et al. (2021) and Arewa and Fahad (2024) have reported that lineaments are essential to the interaction with mineral deposits. They are thought of to offer channels for fluids rich in minerals to build up in the upper crust of the Earth. As a result, lineaments have been widely used in mineral exploration as a useful reference point, and their significance in this sector has been emphasized. A visual observation of the lineament map (Fig. 8) reveals the dominant presence of these structures around the mining sites of Pangu, Wuna, Checheyi and other locations like Kwali, Gwagwalada, Dadabiri, Shanzhi, Suleja, Zuba and Gwarinpa which shows that mineralization potential of the area is structurally controlled. Therefore, these zones of high lineament density are the areas with high mineralisation.

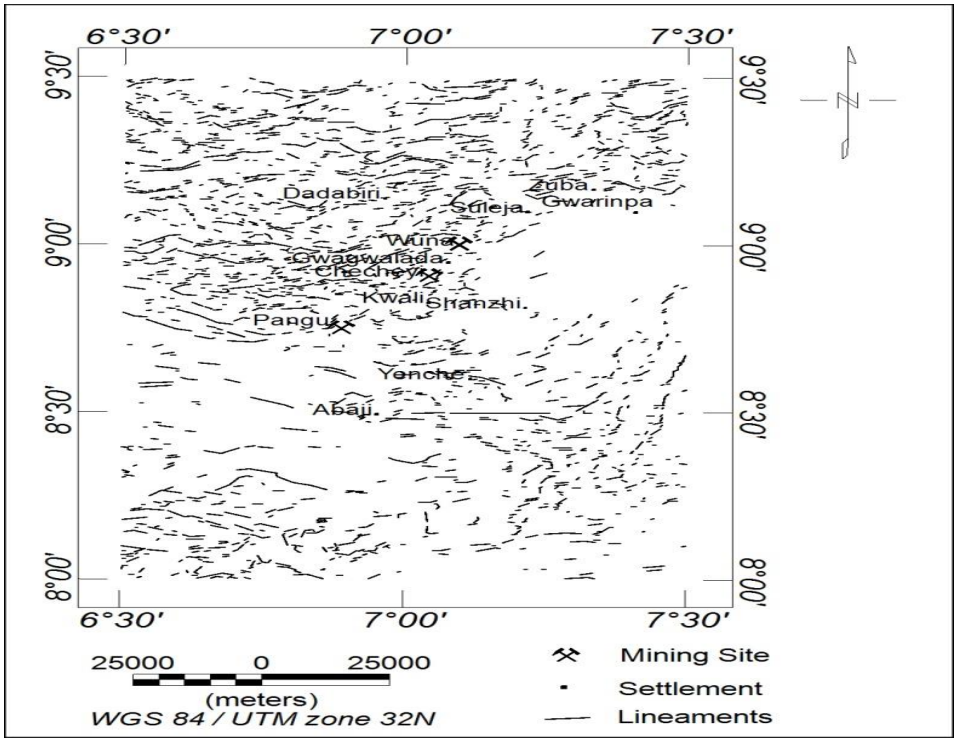

Fig. 9: Lineament map of the study area.

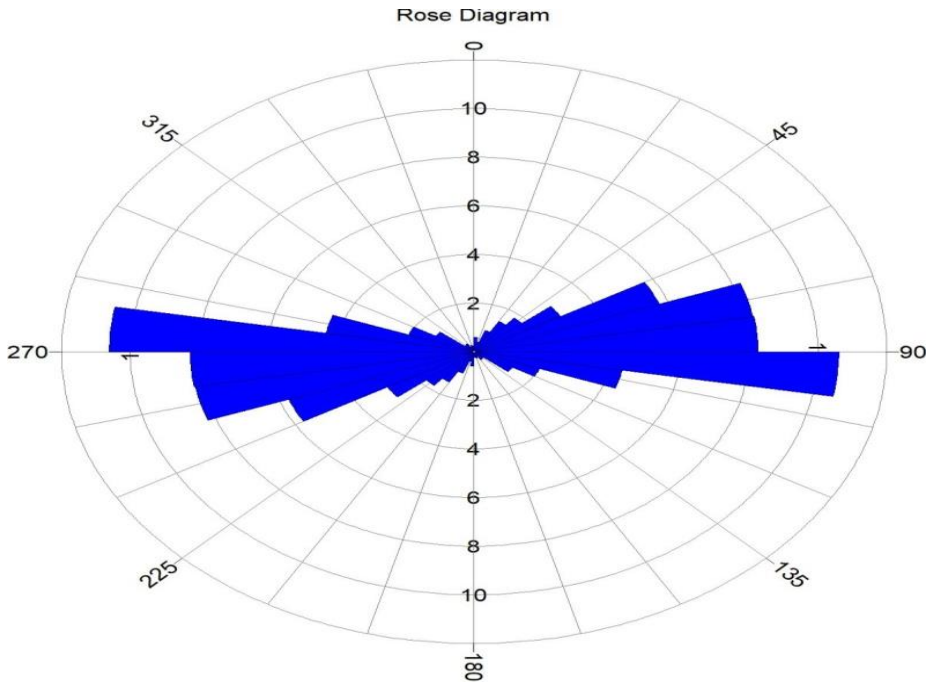

Fig. 10: Rose diagram showing structural trending direction within the study area.

ISSN 2278-2540 | DOI: 10.51583/IJLTEMAS | Volume XIII, Issue V, May 2024

IV. Conclusion

The aeromagnetic data collected over the North-Central Basement Complex area has been interpreted using various filtering techniques. The results suggest the presence of magnetic mineral deposits within this region.

Due to the diverse range of rock types in the area, each with their own unique magnetic susceptibilities, the total magnetic intensity (TMI) map created shows considerable variability in magnetic intensity across the research area. The magnetic intensity values observed within the study region span a range from -99.63 nT to 109.33 nT. The 3-D Euler Deconvolution technique applied revealed the depth of magnetic sources range to be >2000 m, 1000 to 2000 m, 500 to 1000 m, and < 500 m. Most of the highly magnetic structures and intrusive depth sources are within the range of < 100 to 500 m. from the lineament map the predominant directional patterns are shown as E-W, NE-SW, and W-NW to E-SE. Based on the visual observation of the lineament map (Figure 8), the dominant presence of these structures is evident around the mining sites of Pangu, Wuna, Checheyi, as well as other locations like Kwali, Gwagwalada, Dadabiri, Shanzhi, Suleja, Zuba, and Gwarinpa. This suggests that the mineralization potential of the area is structurally controlled which is responsible for localization of gold deposits in the study areas.

Conflict of Interest

Authors declare that they do not have any conflict of interest whatsoever.

Acknowledgement

The authors sincerely appreciate the Nigeria Geological Survey Agency (NGSA) for releasing the data used for the study. The authors also acknowledge the management and staff of Sheda Science and Technology Complex (SHESTCO), Abuja for their moral and for their support

References

1. Abaa, S. I. 1983, “The structure and petrography of alkaline rocks of the Mada Younger Granite Complex, Nigeria”. Journal of African Earth Science, 3, 107–113.
2. Abdulsalam, N. N., Mallam, A. and Likkason O. K. (2011). Identification of Linear Features using continuation filters over Koton Karke area, Nigeria, from Aeromagnetic data. World Rural Observations, 3(1) 1-8.
3. Adetona, A. Abbass And Abu Mallam (2013): Investigating the structures within the Lower Benue and Upper Anambra basins, Nigeria, using first Vertical Derivative, Analytical Signal and (CET) centre for exploration targeting plug-in. Earth Science 2013; 2(5): 104-112.
4. Akande SO, Ojo OJ, Adekeye OA, Ladipo KO, (2006). A Geological Field Duide to the Southern Bida Basin. Nigerian Association of Petroleum Explorationists (NAPE), 24th Annual Conference and Exhibition, Abuja, pp 21.
5. Andrew J., Alkali A., Salako K. A. & Udensi E. E. (2018): Delineating Mineralisation Zones within the Keffi Abuja Area Using Aeromagnetic Data. Journal of Geography, Environment and Earth Science International 15(3): 1-12, 2018; Article no. JGEESI.37052 ISSN: 2454-735.
6. Arifin, M.H., Kayode, J.S., Izwan, M.K., Zaid, H.A. & Hussin, H. (2019): Data for the potential gold mineralisation mapping with the applications of Electrical Resistivity Imaging and Induced Polarization geophysical surveys. Data in belief, 22, 830-835.
7. Arewa James Ogah1 & Fahad Abubakar (2024): Solid mineral potential evaluation using integrated aeromagnetic and aero radiometric datasets. Scientific Reports. 14:1637
8. Bhattachanya, B.K., 1966. Continuous spectrum of the total magnetic field anomaly due to a rectangular prismatic body. Geophysics 31, 97–121.
9. Burke, K., Freeth, S. J. & Grant, N. K. The structure and sequence of geological events in the Basement Complex of the Ibadan area Western Nigeria. Precambrian Res. 3, 537–545 (1976).
10. Dada S. S. (2006). Proterozoic Evolution of Nigeria. In: O. Oshi (Ed.), The Basement Complex of Nigeria and its Mineral Resources (A Tribute to Prof. M. A. O. Rahaman). Akin Jinad & Co. Ibadan, pp29-44.
11. Ejepu J. S., Abdullahi S., Abdulfatai A. I. and Umar M. U. (2020): Predictive Mapping of the Mineral Potential Using Geophysical and Remote Sensing Datasets in Parts of Federal Capital Territory, Abuja, North-Central Nigeria. Earth Sciences 2020; 9(5): 148-163.
12. Faruwa, A. R. et al. Airborne magnetic and radiometric mapping for litho-structural settings and its significance for bitumen mineralization over Agbabu bitumen-belt southwestern Nigeria. J. Afr. Earth Sci. 180, 104222 (2021).
13. Gibert, D. & Galdeano, A. A computer program to perform transformations of gravimetric and aeromagnetic surveys. Comput. Geosci. 11, 553–588 (1985).
14. Guo, W., Dentith, M. C., Xu, J. & Ren, F. Geophysical exploration for gold in Gansu Province, China. Explor. Geophys. 30, 76–82 (1999).
15. Hodges G, Amine D. Exploration for gold deposits with airborne geophysics. KEGS PDAC Symposium; 2010
16. Holden, E. J., Dentith, M. & Kovesi, P. Towards the automated analysis of regional aeromagnetic data to identify regions prospective for gold deposits. Comput. Geosci. 34, 1505–1513 (2008).

ISSN 2278-2540 | DOI: 10.51583/IJLTEMAS | Volume XIII, Issue V, May 2024

17. Holden, E. J. et al. Automated identification of magnetic responses from porphyry systems. ASEG Extend. Abstracts 2010, 1–4 (2010).
18. Ladipo KO (1988). Paleogeography, sedimentation and tectonics of the Upper Cretaceous Anambra Basin, south-eastern Nigeria. J. Afr. Earth Sci. 7:865–871.
19. Lawal, T. O. Integrated aeromagnetic and aero radiometric data for delineating lithologies, structures, and hydrothermal alteration zones in part of southwestern Nigeria. Arab. J. Geosci. 13, 775 (2020).
20. Leu, L. (1982) Use of Reduction-to-the-Equator Process for Magnetic Data Interpretation. Geophysics, 47, 445.
21. MacLeod, I.N., Jones, K., Dai, T.F. 1993. 3-D analytic signal in the interpretation of total magnetic field data at low magnetic latitudes. Exploration Geophysics, 24 (3-4), 679-688.
22. Miller, H. G. & Singh, V. Potential field tilt—A new concept for location of potential field sources. J. Appl. Geophy. 32, 213–217 (1994).
23. Mohammad G. A., Atef A.M. I., Ahmed A. E., Alhussein A. B., Ali M.M. E. & Yara T. (2017): Analysis and interpretation of aeromagnetic data for Wadi Zeidun area, Central Eastern Desert, Egypt. Egyptian Journal of Petroleum 27 (2018) 285–293.
24. Nabighian, M.N. and Hansen, R.O. (2001) Unification of Euler and Werner Deconvolution in Three Dimensions via the Generalized Hilbert Transform. Geophysics, 66, 1805-1810.
25. Nabighian, M.N. (1972): the Analytic Signal of Two-Dimensional Magnetic Bodies with Polygonal Cross-Section: Its Properties and Use for Automated Anomaly Interpretation. Geophysics, 37, 507-517. https://doi.org/10.1190/1.1440276
26. Nabighian, M.N. (1974) Additional Comments on the Analytic Signal of Two Dimensional Magnetic Bodies with Polygonal Cross-Section. Geophysics, 39, 85-92. https://doi.org/10.1190/1.1440416
27. Nigerian Geological Survey Agency. Geology and Structural Lineament Map of Nigeria. Abuja: NGSA; 2006
28. Nigerian Geological Survey Agency, 2010; Airborne Geophysical Digital Data Dissemination Guidelines 1 – 23
29. Nwajide CS (1990). Sedimentation and paleogeography of the Central Benue Trough, Nigeria. In: Ofoegbu, C. O. (Ed.), The Benue Trough Structure and Evolution. Vieweg, Braunschweig, pp19-38.
30. Obaje N. G. (2009). Geology and Mineral Resources of Nigeria. Springer Verlag, Heidelberg (Germany), 240pp.
31. Oguche M., Akanbi, E. S. and O. S. C. (2021): Analysis and interpretation of high resolution aeromagnetic data of Abuja sheet 186 And Gitata sheet 187, Central Nigeria. Science World Journal Vol. 16(No 3) 2021.
32. Onyedim, G. C., Awoyemi, M. O., Ariyibi, E. A., & Arubayi, J. B. (2007). Aeromagnetic imaging of the basement morphology in part of the Middle Benue Trough, Nigeria. Journal of Mining and Geology, 42(2), 157-163. http://dx.doi.org/10.4314/jmg.v42i2.18856
33. Okpoli, C. and Akingboye, A. (2016a). Reconstruction and appraisal of Akunu–Akoko area iron ore deposits using geological and magnetic approaches. RMZ – Materials and Geoenvironment (Materiali in geookolje), 63 (1), 19-38.
34. Oyeniyi, T. O., Salami, A. A. & Ojo, S. B. Magnetic surveying as an aid to geological mapping: A case study from Obafemi Awolowo University Campus in Ile-Ife, Southwest Nigeria. Ife J. Sci. 18, 331–343 (2016).
35. Pettijohn JF (2004). Sedimentary Rocks, 3rd Edition. CBS Publishers and Distributors, New Delhi, pp 628.
36. Priscillia E., Abu M. & Abel. U. O. (2021): Interpretation of Aeromagnetic Data of Part of Gwagwalada Abuja Nigeria for Potential Mineral Targets. Journal of Geological Research | Volume 03 | Issue 04 | October 2021.
37. Reeves, C. (2005). Aeromagnetic Survey Principles, Practice and Interpretation. Geophysics, 1-12.
38. Reid, A. B., Allsop, J. M., Granser, H., Millett, A. J. T. & Somerton, I. W. Magnetic interpretation in three dimensions using Euler deconvolution. Geophysics 55, 80–91 (1990)
39. Roest, W. R., Verhoef, J and Pilkington, M. (1992). Magnetic interpretation using the 3D analytic signal. Geophysics, 57, 116-125.
40. Thompson, D.T. (1973) Identification of Magnetic Source Types Using Equivalent Simple Models. Fall Annual AGU Meeting, San Francisco, 10-13 December 1973.
41. Salem, A., Williams, S., Fairhead, J.D., Ravat, D., and Smith, R. (2007): Tilt-depth method—a simple depth estimation method using first-order magnetic derivatives: The Leading Edge, v. 26, p. 1502-1505.
42. Tsepav M. T. & Abu M. (2017): Evaluation of Depth to Magnetic Basement over Some Parts of the Nupe Basin, Nigeria by Source Parameter Imaging Method using aeromagnetic data. International Journal Science and Research Technology. November 2017 Vol.:8, Issue:1.
43. Wilsher, W.A. (1987) A Structural Interpretation of the Witwatersrand Basin through the Application of Automated Depth Algorithms to Both Gravity and Aeromagnetic Data. M.Sc. Thesis, University of Witwatersrand, Johannesburg.